Directed intermittent search for a hidden target on a dendritic tree

Jay M. Newby[1] and Paul C. Bressloff[1,2]
[1]*Department of Mathematics, University of Utah, Salt Lake City, Utah 84112, USA*
[2]*Mathematical Institute, University of Oxford, 24-29 St. Giles, Oxford OX1 3LB, United Kingdom*
(Received 4 June 2009; published 13 August 2009)

Motivated by experimental observations of active (motor-driven) intracellular transport in neuronal dendrites, we analyze a stochastic model of directed intermittent search on a tree network. A particle injected from the cell body or soma into the primary branch of the dendritic tree randomly switches between a stationary search phase and a mobile nonsearch phase that is biased in the forward direction. A (synaptic) target is presented somewhere within the tree, which the particle can locate if it is within a certain range and in the searching phase. We approximate the moment generating function using Green's function methods. The moment generating function is then used to compute the hitting probability and conditional mean first passage time to the target. We show that in contrast to a previously explored finite interval case, there is a range of parameters for which a bidirectional search strategy is more efficient than a unidirectional one in finding the target.

DOI: 10.1103/PhysRevE.80.021913 PACS number(s): 87.16.A−, 87.19.L−, 87.10.−e

I. INTRODUCTION

Recently, a stochastic model of intermittent random search has been developed [1–3] where a Markov process governs the internal state of a particle moving on a one-dimensional track (or its higher–dimensional generalization). The internal states consist of a forward moving state, a backward moving state, and a stationary (or diffusing) searching state. There is a target of unknown location somewhere along the track, which absorbs the particle at a certain rate if the particle is within a certain range of the target and is in the searching state. The random motion is taken to be unbiased with periodic or reflecting boundary conditions, which ensures that the particle will eventually find the target. The efficiency of the random search is characterized by minimizing the mean first passage time to the target with respect to the state transition rates. Models of intermittent random search have been applied to a wide range of biological problems including animal foraging [1,4,5] and DNA binding kinetics [6,7].

Intermittent random search can also be used to model active (motor-driven) cargo transport along microtubules and subsequent delivery to subcellular synaptic compartments within neurons [8,9]. Recently, there has much interest in microtubule transport in both axons and dendrites as this process plays an important role in synaptic plasticity and many neurological disorders [10–12]. However, in contrast to previous applications of random intermittent search, active transport tends to be biased in a certain direction. Additionally, when considering cargo delivery to synaptic sites within an axon or dendrite, many possible outcomes exist. For example, the cargo could be localized to one of many different possible sites, or it could be degraded. Thus, to model active cargo transport and delivery in the neuron as an intermittent random search, we must consider biased motion and a nonzero probability of failure to find a particular target.

Biased motion implies two different types of search strategy: a unidirectional strategy with only one forward moving state, and a bidirectional strategy with two moving states. Experiments have shown both unidirectional and bidirectional cargo transports within neuronal axons and dendrites [13–16]. In our previous paper [8], we considered both strategies on a finite interval with a reflecting boundary at the starting location and an absorbing boundary at the other end of the interval. Since a unidirectional strategy only has one shot at finding the target it must spend as much time as possible in the searching state at the expense of taking longer to reach the target. The goal was to find out if bidirectional motion could improve upon the unidirectional strategy by allowing the particle to back up after missing the target. To explore this possibility we calculated both the hitting probability and the conditional mean first passage time (MFPT) to the target. We compared the two strategies by fixing the hitting probability and comparing their MFPT to see which could find the target faster. Our analysis showed that under these constraints, the unidirectional search strategy will always find the target faster than the bidirectional search strategy.

In this paper we extend our previous work on directed intermittent search in order to take into account the extensive branching structure of a neuron's dendrites [17]. We use this to show that, in contrast to a finite interval, partially biased bidirectional transport can be more efficient than unidirectional transport on a tree network. This is consistent with the intuitive idea that if a transported cargo goes down an incorrect branch, a bidirectionally moving cargo can back up and go down the correct branch, whereas a unidirectionally moving cargo must keep moving forward along the incorrect branch; the cost of such overshooting is amplified in the presence of branching. Our analytical results offer a possible explanation for the different dynamical behaviors observed in neuronal microtubular cargo transport [13–16]. We also establish that branching leads to an exponential reduction in the probability of finding a distant target, suggesting that more local search strategies are necessary. This is consistent with the finding that clusters of immobile transport vesicles are found at branch nodes along the dendritic tree.

In order to handle the additional complexity arising from branching, we first carry out a quasi-steady-state reduction in

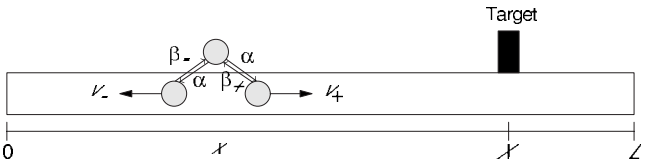

FIG. 1. Schematic diagram of the stochastic directed intermittent search model.

the master equation of the full three-state Markov model, which leads to a scalar Fokker-Planck equation (Sec. II). We previously applied such a reduction to a general class of molecular motor-based models of cargo transport, and showed that it approximates the hitting probability and MFPT on a finite interval to a high degree of accuracy [9]. We then construct the Laplace transformed Green's function of the Fokker-Plank (FP) equation on a tree network by adapting a method previously used to calculate the Green's function of the advection-diffusion equation [18–20] (Sec. III). Having obtained the Green's function on a tree, the problem of computing the hitting probability and MFPT reduces to solving a single integral equation, which can be approximated numerically and analytically. We illustrate our Green's function construction using two simple examples: a single branch node and a semi-infinite Cayley tree (Sec. IV). Finally, we calculate the hitting probability and MFPT to find a hidden target on a tree, and use this to determine the effects of branching on the efficiency of the directed intermittent search strategy (Sec. V).

II. STOCHASTIC MODEL OF DIRECTED INTERMITTENT SEARCH

In our previous work [8], we introduced a three-state directed intermittent random search model in which a particle moving along a one-dimensional track of length L can be in one of three internal states: Forward moving with velocity v_+, backward moving with velocity v_-, and searching with zero velocity. The target located at X can be detected if the particle is within a distance l of the target and in the searching state (see Fig. 1).

The transitions between the three internal states are governed by a Markov process. Let $Z(t)$ and $N(t)$ denote the random position and state of the particle at time t and define $\mathbb{P}(x,t,n|y,0,m)dx$ as the joint probability that $x \leq Z(t) < x+dx$ and $N(t)=n$ given that initially the particle was at position $Z(0)=y$ and was in state $N(0)=m$. Setting

$$p_n(x,t) \equiv \mathbb{P}(x,t,n|0,0,+) \tag{2.1}$$

with initial condition $p_n(x,0)=\delta(x)\delta_{n,+}$, we have the following master equation describing the evolution of the probability densities for $t>0$:

$$\partial_t p_+ = -v_+\partial_x p_+ - \beta_+ p_+ + \alpha p_0, \tag{2.2a}$$

$$\partial_t p_- = v_-\partial_x p_- - \beta_- p_- + \alpha p_0, \tag{2.2b}$$

$$\partial_t p_0 = \beta_+ p_+ + \beta_- p_- - 2\alpha p_0 - \kappa\chi([x-X]/l)p_0, \tag{2.2c}$$

where the indicator function χ is defined by

$$\chi(x) = \begin{cases} 1, & |x| < 1 \\ 0, & \text{otherwise.} \end{cases} \tag{2.3}$$

Here $\alpha, \beta_\pm$ are the transition rates between the stationary and mobile states as indicated in Fig. 1. Master Eq. (2.1) is supplemented by a reflecting boundary condition at $x=0$ and an absorbing boundary condition at $x=L$. That is,

$$p_-(0,t) = p_+(0,t), \quad p_-(L,t) = 0. \tag{2.4}$$

The absorbing boundary takes into account the fact that transported cargo can be degraded or absorbed by other targets downstream to the given target. Finally, we assume that the bidirectional transport is partially biased in the forward moving (anterograde) direction by taking $v_-/\beta_- < v_+/\beta_+$, which implies that when $v_+=v_-$ the particle spends more time in the anterograde state than the backward moving (retrograde) state. Unidirectional transport is obtained in the limit $\beta_- \to \infty$, whereas unbiased bidirectional transport occurs when $v_-/\beta_- = v_+/\beta_+$.

Suppose that we nondimensionalize master Eq. (2.1) by rescaling space and time according to

$$x \to \frac{x}{l}, \quad t \to t\frac{v_-}{l},$$

where l is the typical size of the target. Assuming that the transition rates $\alpha, \beta_\pm$ are large compared to v_+/l, we introduce the dimensionless parameters $k=\kappa l/v$, $v=v_-/v_+$, $a=\epsilon\alpha l/v_+$, and $b_\pm=\epsilon\beta_\pm l/v_+$, where $\epsilon \ll 1$. Master Eq. (2.1) then becomes

$$\partial_t p_+ = \frac{1}{\epsilon}(-b_+ p_+ + a p_0) - \partial_x p_+, \tag{2.5a}$$

$$\partial_t p_- = \frac{1}{\epsilon}(-b_- p_- + a p_0) + v\partial_x p_-, \tag{2.5b}$$

$$\partial_t p_0 = \frac{1}{\epsilon}(b_+ p_+ + b_- p_- - 2a p_0) - k\chi(x-X)p_0. \tag{2.5c}$$

We previously presented a method for reducing this set of master equations to a single second-order scalar equation for u defined as the total probability of being at position x at time t in any of the three states [9]. This reduction is motivated by the small parameter $\epsilon \ll 1$ causing the underlying Markov process to evolve quickly toward its stable steady-state distribution. The probabilities p_n will be constantly perturbed off this stable manifold as information propagates forward and backward at the characteristic speeds 1, $-v$. Using perturbation methods along the lines of those presented in [21] we can reduce the system of three scalar master equations to a single second-order scalar equation for u. Note that a number of authors have previously carried out a quasi-steady-state reduction in linear reaction-hyperbolic equations such as Eq. (2.4), but have focused on the wavelike properties of the transport process in the absence of a hidden target [22–24].

We first rewrite the master equation in the matrix form

$$\partial_t \mathbf{p} = \frac{1}{\epsilon} A\mathbf{p} + \mathcal{L}(\mathbf{p}), \tag{2.6}$$

where $p=(p_+,p_-,p_0)^T$, A is the matrix

$$A = \begin{bmatrix} -b_+ & 0 & a \\ 0 & -b_- & a \\ b_+ & b_- & -2a \end{bmatrix}, \tag{2.7}$$

and $\mathcal{L}$ is the linear operator

$$\mathcal{L}(\mathbf{f}) = \begin{bmatrix} -\partial_x f_1 \\ v\partial_x f_2 \\ -k\chi(x-X)f_3 \end{bmatrix}. \tag{2.8}$$

The left null space of the matrix A is spanned by the vector

$$\psi = \begin{pmatrix} 1 \\ 1 \\ 1 \end{pmatrix}, \tag{2.9}$$

and the right null space is spanned by

$$\mathbf{p}^{ss} = \frac{1}{\gamma}\begin{pmatrix} \frac{1}{b_+} \\ \frac{1}{b_-} \\ \frac{1}{a} \end{pmatrix}. \tag{2.10}$$

The normalization factor γ is chosen so that $\psi^T\mathbf{p}^{ss}=1$, that is,

$$\gamma = \frac{1}{b_+} + \frac{1}{b_-} + \frac{1}{a}. \tag{2.11}$$

Let $u=\psi^T\mathbf{p}$ and $\mathbf{w}=\mathbf{p}-u\mathbf{p}^{ss}$ such that $\psi^T\mathbf{w}=0$. We can interpret u as the component of $\mathbf{p}$ in the left null space of A, whereas $\mathbf{w}$ is in the orthogonal complement.

Multiplying both sides of Eq. (2.6) by ψ^T we obtain

$$\partial_t u = \psi^T \mathcal{L}(u\mathbf{p}^{ss} + \mathbf{w}). \tag{2.12}$$

Substituting $\mathbf{p}=\mathbf{w}+u\mathbf{p}^{ss}$ into Eq. (2.6) yields

$$\partial_t \mathbf{w} + \partial_t u\mathbf{p}^{ss} = \frac{1}{\epsilon} A(\mathbf{w} + u\mathbf{p}^{ss}) + \mathcal{L}(\mathbf{w} + u\mathbf{p}^{ss}). \tag{2.13}$$

Using the fact that $\mathbf{p}^{ss}$ is in the right null space of A and using Eq. (2.12) in the above equation we obtain

$$\partial_t \mathbf{w} = \frac{1}{\epsilon} A\mathbf{w} + (\mathbb{I}_3 - \mathbf{p}^{ss}\psi^T)\mathcal{L}(\mathbf{w} + u\mathbf{p}^{ss}), \tag{2.14}$$

where $\mathbb{I}_3$ is the 3×3 identity matrix. Now introduce the asymptotic expansion for $\mathbf{w}$

$$\mathbf{w} \sim \mathbf{w}_0 + \epsilon\mathbf{w}_1 + \epsilon^2\mathbf{w}_2 + \cdots. \tag{2.15}$$

After substituting this expansion into Eq. (2.14) and collecting $O(\epsilon^{-1})$ terms we obtain the equation for $\mathbf{w}_0$

$$A\mathbf{w}_0 = 0. \tag{2.16}$$

By construction $\mathbf{w}$ is in the orthogonal complement to the left null space of A, it follows that $\mathbf{w}_0=0$. Now collecting terms of $O(1)$ yields the equation

$$A\mathbf{w}_1 = -(\mathbb{I}_3 - \mathbf{p}^{ss}\psi^T)\mathcal{L}(u\mathbf{p}^{ss}). \tag{2.17}$$

Although the matrix A is singular the orthogonal projection operator $(\mathbb{I}_3-\mathbf{p}^{ss}\psi^T)$ ensures that the right-hand side of the above equation is in the range of A. By the Fredholm alternative theorem a solution $\mathbf{w}_1$ exists. This rank 2 system can be solved up to the arbitrary element $w_{0,1}$ using Gaussian elimination. We have the following asymptotic expansion to first order in ϵ:

$$\mathbf{w} \sim \epsilon\begin{pmatrix} \frac{k\chi(x-X)}{ab_+^2\gamma^2}u - \frac{1-V_0}{b_+^2\gamma}\partial_x u + \frac{a\Omega}{b_+} \\ \frac{k\chi(x-X)}{ab_-^2\gamma^2}u + \frac{v+V_0}{b_-^2\gamma}\partial_x u + \frac{av\Omega}{b_-} \\ \Omega \end{pmatrix}, \tag{2.18}$$

where we have set $\Omega=w_{0,1}$ and

$$V_0 = \frac{1}{\gamma}\left(\frac{1}{b_+} - \frac{v}{b_-}\right).$$

We can determine Ω by imposing the condition $\psi^T\mathbf{w}=0$. This yields

$$a\Omega = -\frac{k\chi(x-X)}{a\gamma^3}\left(\frac{1}{b_+^2} + \frac{1}{b_-^2}\right)u + \frac{1}{\gamma^2}\left(\frac{1-V_0}{b_+^2} - \frac{v+V_0}{b_-^2}\right)\partial_x u. \tag{2.19}$$

Substituting this into Eq. (2.14) yields the FP equation

$$\frac{\partial u}{\partial t} = -\Lambda u - V\frac{\partial u}{\partial x} + D\frac{\partial^2 u}{\partial x^2}, \tag{2.20}$$

where $\Lambda=\lambda\chi(x-X)$ and

$$\lambda = \frac{k}{a\gamma} + \epsilon\frac{k^2}{a^2\gamma^3}\left(\frac{1}{b_+^2} + \frac{1}{b_-^2}\right), \tag{2.21}$$

$$V = V_0 + \epsilon\frac{k\chi(x-X)}{a\gamma^2}\left(\frac{1}{b_+^2} - \frac{1}{b_-^2} + \frac{1-2V_0}{b_+^2} - \frac{1+2V_0}{b_-^2}\right), \tag{2.22}$$

$$D = \epsilon\left(\frac{(1-V_0)^2}{\gamma b_+^2} + \frac{(v+V_0)^2}{\gamma b_-^2}\right). \tag{2.23}$$

The leading-order behavior is obtained by taking $\lambda=\lambda_0=k/a\gamma$ and $V=V_0$. The probability density function u is the total probability of being in any motor state at position x and time t, given that the particle was initially injected onto the track at $x=0$. We use equilibrium initial conditions, so that the process always starts on the slow manifold. The reflecting boundary at $x=0$ yields the boundary condition

$$\left(D\frac{\partial u}{\partial x}-Vu\right)\Big|_{x=0}=0. \tag{2.24}$$

In the following section we use Laplace transform and Green's function methods to solve the Fokker-Planck Eq. (2.20) on both a finite interval and a tree network, in order to compute observable quantities that will allow us to characterize how the efficiency of the random search depends on network topology.

III. CALCULATION OF HITTING PROBABILITY AND MFPT USING GREEN'S FUNCTIONS

The efficiency of the random search can be characterized in terms of the probability of finding the target which we will refer to as the hitting probability Π, and the conditional mean first passage time to the target T. An optimal search strategy (if it exists) is given by the set of transition rates $\alpha,\beta_{\pm}$ which maximize Π and minimize T. Let $\mathbb{P}(t)=\int_0^L u(x,t)dx$ be the total probability that the particle is still located in the domain $0<x<L$ at time t. Integrating Eq. (2.20) with respect to x and using boundary conditions (2.24), we have

$$\frac{\partial \mathbb{P}}{\partial t}=-\lambda\int_{X-1}^{X+1}u(x,t)dx+\left(D\frac{\partial u}{\partial x}-Vu\right)\Big|_{x=L}. \tag{3.1}$$

It follows that the total flux into the target is

$$J(t)=\lambda\int_{X-1}^{X+1}u(x,t)dx. \tag{3.2}$$

The hitting probability, having started at $x=0$ at time $t=0$, is then

$$\Pi=\int_0^{\infty}J(t)dt, \tag{3.3}$$

and the corresponding conditional MFPT is

$$T=\frac{\int_0^{\infty}tJ(t)dt}{\int_0^{\infty}J(t)dt}. \tag{3.4}$$

Consider the Laplace transform of the probability flux J,

$$\Upsilon(s)\equiv\tilde{J}(s)=\int_0^{\infty}e^{-st}J(t)dt. \tag{3.5}$$

Taylor expanding the integral with respect to the Laplace variable s shows that

$$\Upsilon(s)=\int_0^{\infty}J(t)[1-st+s^2t^2/2-\cdots]$$
$$=\Pi\left[1-sT+\frac{s^2}{2}T^{(2)}-\cdots\right], \tag{3.6}$$

assuming that the moments

$$T^{(n)}=\frac{\int_0^{\infty}t^nJ(t)dt}{\int_0^{\infty}J(t)dt} \tag{3.7}$$

are finite. Thus, $\Upsilon(s)$ can be viewed as a generating function for the moments of the conditional first passage time distribution [25]. Equations (3.2) and (3.5) imply that

$$\Upsilon(s)=\lambda\int_{-1}^{1}\tilde{U}(x+X,s)dx, \tag{3.8}$$

where $\tilde{U}(x,s)$ is the Laplace transform of $u(x,t)$. Hence, we can proceed by solving the Laplace transformed Fokker-Planck equation to determine $\tilde{U}(x,s)$. Substituting the result into Eq. (3.8) and Taylor expanding with respect to s then allows us to extract Π and T using Eq. (3.6).

Laplace transforming Eq. (2.20) under the initial condition $u(x,0)=\delta(x)$ gives

$$D\partial_x^2\tilde{U}(x,s)-V\partial_x\tilde{U}(x,s)-s\tilde{U}(x,s)=\lambda\chi(x-X)\tilde{U}(x,s)-\delta(x). \tag{3.9}$$

The associated Green's function $\mathcal{G}(x,y;s)$ satisfies

$$[D\partial_x^2-V\partial_x-s]\mathcal{G}(x,y;s)=\delta(x-y) \tag{3.10}$$

with homogeneous boundary conditions. The Green's function can be used to convert Eq. (3.9) into the integral equation

$$\tilde{U}(x,s)-\lambda\int_{-1}^{1}\mathcal{G}(x,y+X;s)\tilde{U}(y+X,s)dy=-\mathcal{G}(x,0;s). \tag{3.11}$$

A particularly useful aspect of the integral equation representation is that it can be extended to a general tree network by constructing the corresponding network Green's function. We will calculate the latter by introducing inhomogeneous boundary conditions at the branch nodes of the tree and solving the Green's function on each branch separately. The solutions are then matched by imposing current conservation at each branch node and using an iterative procedure to express the Green's function as a continued fraction, following along similar line to a previous analysis of the drift-diffusion equation on a tree [18–20]. This method of calculating the Green's function is related to the graphical calculus developed by several authors within the context of linear cable theory [26–29]. An alternative approach to calculating the Green's function is based on the so-called "sum-over-trips" formalism [30–34], which generates an infinite series expansion of the Green's function on a tree using the method of images. Truncating this series expansion for sufficiently large s and carrying out a numerical inversion of the Laplace transform generates an approximate solution for the corresponding real-time Green's function, which is valid up to some finite time t. In this paper, however, we are interested in the small-s behavior of the Green's function and the associated generating function, see Eq. (3.6), and so we will fol-

low the continued fraction method here. Since our calculations of the Green's function will be for fixed s and y, we will tend to suppress the explicit dependence on these variables for ease of notation.

A. Finite interval Green's function

We first determine the Green's function on a finite interval satisfying Eq. (3.10) subject to the homogeneous boundary conditions (suppressing the s dependence)

$$A_0 \frac{\partial}{\partial x}\mathcal{G}(0,y) - B_0 \mathcal{G}(0,y) = 0, \tag{3.12}$$

$$A_L \frac{\partial}{\partial x}\mathcal{G}(L,y) - B_L \mathcal{G}(L,y) = 0. \tag{3.13}$$

These reduce to Dirichlet or closed boundary conditions when $A_{0,L}=0$ and Neumann or closed boundary conditions when $B_{0,L}=0$. Using standard methods, the Green's function is given by

$$\mathcal{G}(x,y) = \frac{1}{DW(y)} \begin{cases} \psi^{(0)}(x)\psi^{(L)}(y), & 0 \le x \le y \\ \psi^{(L)}(x)\psi^{(0)}(y), & y \le x \le L, \end{cases} \tag{3.14}$$

where

$$\psi^{(0)}(x) = (\mu_2 A_0 - B_0)e^{\mu_1 x} - (\mu_1 A_0 - B_0)e^{\mu_2 x}, \tag{3.15}$$

$$\psi^{(L)}(x) = (\mu_2 A_L - B_L)e^{\mu_1 (x-L)} - (\mu_1 A_L - B_L)e^{\mu_2 (x-L)}, \tag{3.16}$$

$$W(y) = \psi^{(0)}(y)\psi^{(L)\prime}(y) - \psi^{(0)\prime}(y)\psi^{(L)}(y). \tag{3.17}$$

The implicit s dependence of the Green's function arises from the eigenvalues

$$\mu_{1,2} = \frac{V \pm \sqrt{V^2 + 4Ds}}{2D}. \tag{3.18}$$

To obtain the Green's function for two open boundaries we set $A_{0,L}=0$ and $B_{0,L}=-1$ to get

$$\mathcal{G}^{+}(x,y) = \begin{cases} \dfrac{\psi(x)\psi(y-L)}{DW^{+}(y)}, & 0 \le x \le y \\ \dfrac{\psi(x-L)\psi(y)}{DW^{+}(y)}, & y \le x \le L, \end{cases} \tag{3.19}$$

where

$$\psi(x) = e^{\mu_1 x} - e^{\mu_2 x} \tag{3.20}$$

$$W^{+}(y) = \psi(y)\psi'(y-L) - \psi'(y)\psi(y-L). \tag{3.21}$$

For a left closed boundary and a right open boundary the Green's function can be obtained by setting $A_0=D$, $B_0=V$, $A_L=0$, and $B_L=-1$ to get

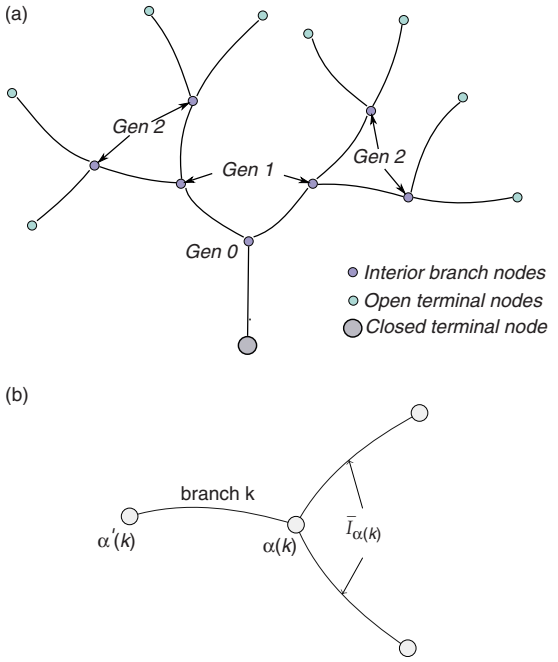

FIG. 2. (Color online) Labeling scheme for a general dendritic tree. (a) An example of a tree Γ with three generations (Gen) of branch nodes, a primary closed terminal node (corresponding to the soma), and a set of open terminal nodes. (b) The branch node $\alpha(k)$ is shown in relation to the neighboring branch node $\alpha'(k)$ closest to the primary node. The branch segments extending out from $\alpha(k)$ in the positive direction together comprise the set $\bar{\mathcal{I}}_{\alpha(k)}$.

$$\mathcal{G}^{-}(x,y) = \begin{cases} \dfrac{\phi(x)\psi(y-L)}{DW^{-}(y)}, & 0 \le x \le y \\ \dfrac{\psi(x-L)\phi(y)}{DW^{-}(y)}, & y \le x \le L, \end{cases} \tag{3.22}$$

where

$$\phi(x) = (\mu_2 D - V)e^{\mu_1 x} - (\mu_1 D - V)e^{\mu_2 x}, \tag{3.23}$$

$$W^{-}(y) = \phi(y)\psi'(y-L) - \phi'(y)\psi(y-L). \tag{3.24}$$

B. Green's function for a general tree

Let us now consider an arbitrary tree Γ, which is assumed to be finite (we consider an infinite tree in Sec IV B), consisting of N_v nodes or vertices and N_e line segments or edges [see Fig. 2(a)]. External line segments are assumed to be finite in length, although generalizing this procedure to account for infinite external line segments is straightforward. The nodes $\alpha \in \Gamma$ of the network may be classified as either branching or terminal. Let $\mathcal{B}$ denote the set of branching nodes, and let $\mathcal{O}$ and $\mathcal{C}$ denote the set of terminal nodes (on external line segments) with open and closed boundary conditions, respectively. We will take the primary terminal node (corresponding to the soma of a neuron) to be closed and all other terminal nodes to be open. The first branch node opposite the closed terminal node is denoted by α_0. For every other branching node $\alpha \in \mathcal{B}$ and open terminal node $\alpha \in \mathcal{O}$,

there exists a unique direct path from α_0 to α (one that does not traverse any line segment more than once). We can label each node $\alpha \neq \alpha_0$ uniquely by the index k of the final segment of the direct path from α_0 to α so that the branch node corresponding to a given segment label k can be written $\alpha(k)$. We denote the other node of segment k by $\alpha'(k)$. For example, α_0' is the single closed terminal node. We can also introduce a direction on each segment of the tree such that every direct path from α_0' always moves in the positive direction. Consider a single branching node $\alpha \in \mathcal{B}$ and label the set of segments radiating from it by $\mathcal{I}_\alpha$. Let $\bar{\mathcal{I}}_\alpha$ denote the set of line segments $k \in \mathcal{I}_\alpha$ that radiate from $\alpha \in \mathcal{B}$ in a positive direction [see Fig. 2(b)]. If we denote the total number of segments radiating from any branch node α by the coordination number z, then the number of elements of $\mathcal{B}_\alpha$ is $z-1$. (Motivated by the example of branching axons and dendrites, we take the coordination number of the tree to be $z=3$). Using these various definitions we can introduce the idea of a generation. Take α_0 to be the zeroth generation. The first generation then consists of the set of nodes $\Sigma_1 = \{\alpha(k), k \in \bar{\mathcal{I}}_{\alpha_0}\}$, the second generation is $\Sigma_2 = \{\alpha(l), l \in \bar{\mathcal{I}}_\alpha, \alpha \in \Sigma_1\}$, etc. Let N denote the maximum number of generations, that is, N is the smallest integer for which Σ_{N+1} only includes terminal nodes.

Denote the position coordinate along the ith line segment by x, $0 \leq x \leq L_i$, where L_i is the length of the segment and $1 \leq i \leq N_e$. Given the above labeling scheme for nodes, we take $x(\alpha'(i))=0$ and $x(\alpha(i))=L$. Let u_i denote the probability density on the ith segment, which evolves according to the FP equation

$$\frac{\partial u_i}{\partial t} = D_i \frac{\partial^2 u_i}{\partial x^2} - V_i \frac{\partial u_i}{\partial x}, \quad 0 < x < L_i, \tag{3.25}$$

where D_i is the diffusion constant and V_i is the drift velocity on the ith segment. For the moment, we are ignoring the effects of absorption by a hidden target on one of the branches. Equation (3.25) is supplemented by the initial condition

$$u_i(x,0) = \delta_{i,0}\delta(x), \tag{3.26}$$

assuming that the particle starts at the closed terminal node (labeled $i=0$), together with a set of boundary conditions at terminal and branch nodes. Let $\mathcal{J}_i[u_i]$ denote the corresponding probability current or flux, which is taken to be positive in the direction flowing away from the primary node at the soma,

$$\mathcal{J}_i[u] \equiv -D_i \frac{\partial u_i}{\partial x} + V_i u_i. \tag{3.27}$$

The closed boundary condition on the primary terminal branch is

$$\mathcal{J}_0[u](0,t) = 0, \tag{3.28}$$

whereas the open boundary condition at all other terminal segments is

$$u_i(L_i,t) = 0 \quad \text{for} \quad \alpha(i) \in O/\{\alpha_0'\}. \tag{3.29}$$

At all branch nodes $\alpha \in \mathcal{B}$ we impose the continuity conditions

$$u_i(x(\alpha),t) = \Phi_\alpha(t), \quad \text{for all} \quad i \in \mathcal{I}_\alpha, \tag{3.30}$$

where the $\Phi_\alpha(t)$ are unknown functions, which will ultimately be determined by imposing current conservation at each branch node,

$$\sum_{i \in \mathcal{I}_\alpha} \mathcal{J}_i[u](x(\alpha),t) = 0. \tag{3.31}$$

Note that for the upstream segment $j \notin \bar{\mathcal{I}}_\alpha$, $x(\alpha)=L_j$ and the corresponding flux $\mathcal{J}_j[u](L_j,t)$ flows into the branch node, whereas for the remaining $z-1$ downstream segments $k \in \bar{\mathcal{I}}_\alpha$, we have $x(\alpha)=0$ and the flux $\mathcal{J}_k[u](0,t)$ flows out of the branch node.

Suppose that we now have a hidden target of half-width $l=1$ and position X on the jth branch such that $1 < X < L_j - 1$. (The lower and upper bounds are chosen so that all of the target is contained within the segment). After Laplace transforming the above system of equations on a tree, we obtain the integral equation

$$\tilde{U}_i(x,s) - \lambda \int_{-1}^{1} G_{i,j}(x, y+X; s)\tilde{U}_j(y,s)dy = -G_{i,0}(x,0;s), \tag{3.32}$$

where $G_{i,j}$ is the corresponding Green's function on the tree

$$\left[D_i \frac{\partial^2}{\partial x^2} - V_i \frac{\partial}{\partial x} - s \right] G_{i,j}(x,y;s) = \delta_{i,j}\delta(x-y). \tag{3.33}$$

Given a target on the jth branch, the generating function for the hitting probability and MFPT is

$$\Upsilon_j(s) = \lambda \int_{-1}^{1} \tilde{U}_j(x+X,s)dx. \tag{3.34}$$

The fundamental solution in each branch is given by the corresponding finite interval Green's function supplemented by terms satisfying inhomogeneous boundary conditions of form (3.30). For internal branches i (suppressing the s variable),

$$G_{i,j}(x,y) = \delta_{i,j}\mathcal{G}_i^+(x,y) + \Phi_{\alpha'(i)}(y)\hat{F}_i(x) + \Phi_{\alpha(i)}(y)F_i(x), \tag{3.35}$$

for all open terminal branches ($i \neq 0$)

$$G_{i,j}(x,y) = \delta_{i,j}\mathcal{G}_i^+(x,y) + \Phi_{\alpha'(i)}(y)\hat{F}_i(x), \tag{3.36}$$

and for $i=0$

$$G_{0,j}(x,y) = \delta_{0,j}\mathcal{G}_0^-(x,y) + \Phi_{\alpha_0}(y)F_0(x). \tag{3.37}$$

Here $\mathcal{G}_i^+$ and $\mathcal{G}_i^-$ are Green's functions (3.19) and (3.22) on the ith branch. The functions $F_k(x)$, $\hat{F}_k(x)$, $k \neq 0$ satisfy the Laplace transformed FP equation with boundary conditions $F_k(0)=0$, $F_k(L_k)=1$ and $\hat{F}_k(0)=1$, $\hat{F}_k(L_k)=0$,

$$F_k(x) = \frac{\psi_k(x)}{\psi_k(L_k)}, \quad \hat{F}_k(x) = \frac{\psi_k(x-L_k)}{\psi_k(-L_k)} \tag{3.38}$$

with $\psi_k(x)$ the k-dependent form of $\psi(x)$, Eq. (3.20),

$$\psi_k(x) = 2e^{V_k x/2D_k}\sinh(\eta_k x), \tag{3.39}$$

$$\eta_k = \sqrt{\left(\frac{V_k}{2D_k}\right)^2 + \frac{s}{D_k}}. \tag{3.40}$$

For $k=0$ we have

$$F_0(x) = \frac{\phi_0(x)}{\phi_0(L_0)}, \tag{3.41}$$

with $\phi_0(x)$ given by Eq. (3.23) for $D=D_0$, $V=V_0$, and $L=L_0$. The unknown functions Φ_α are determined by imposing current conservation condition (3.31) at each branch node and using the identity $\mathcal{J}_j[\Phi_\alpha F]=\Phi_\alpha \mathcal{J}_j[F]$, which follows from the observation that Φ_α is x independent. At the zeroth generation node α_0, the current conservation equation is given by (suppressing the s and y variables)

$$\Phi_{\alpha_0}\mathcal{J}_0[F](L_0) = \sum_{k\in\bar{\mathcal{I}}_{\alpha_0}} \Phi_{\alpha(k)}\mathcal{J}_k[F](0) + \Phi_{\alpha_0}\sum_{k\in\bar{\mathcal{I}}_{\alpha_0}} \mathcal{J}_k[\hat{F}](0) + \mathcal{X}_{\alpha_0}, \tag{3.42}$$

and at all other branching nodes $\alpha(p)\in\Sigma_n$, $1\le n<N$ we have

$$\Phi_{\alpha'(p)}\mathcal{J}_p[\hat{F}](L_p) + \Phi_{\alpha(p)}\mathcal{J}_p[F](L_p) = \sum_{k\in\bar{\mathcal{I}}_{\alpha(p)}} \Phi_{\alpha(k)}\mathcal{J}_k[F](0) + \Phi_{\alpha(p)}\sum_{k\in\bar{\mathcal{I}}_{\alpha(p)}} \mathcal{J}_k[\hat{F}](0) + \mathcal{X}_{\alpha(p)}, \tag{3.43}$$

where the target location dependent terms are defined according to

$$\mathcal{X}_{\alpha_0} \equiv \sum_{k\in\bar{\mathcal{I}}_{\alpha_0}} \mathcal{J}_k[\mathcal{G}^+](0)\delta_{k,j} - \mathcal{J}_0[\mathcal{G}^-](L_0)\delta_{0,j} \tag{3.44}$$

and

$$\mathcal{X}_{\alpha(p)} \equiv \sum_{k\in\bar{\mathcal{I}}_{\alpha(p)}} \mathcal{J}_k[\mathcal{G}^+](0)\delta_{k,j} - \mathcal{J}_p[\mathcal{G}^+](L_p)\delta_{p,j}. \tag{3.45}$$

Note that $\mathcal{X}_\alpha$ depends on the source location y through its dependence on the finite interval Green's functions $\mathcal{G}^\pm$; this then generates the y dependence of the functions Φ_α

The four possible contributions to the probability flux at any branch $k\neq 0$ are

$$g_k \equiv \mathcal{J}_k[\hat{F}](L_k) = \frac{D_k\eta_k e^{V_k L_k/2D_k}}{\sinh(\eta_k L)}, \tag{3.46}$$

$$h_k \equiv \mathcal{J}_k[F](L_k) = -D_k\eta_k\coth(\eta_k L_k) + \frac{V_k}{2}, \tag{3.47}$$

$$\bar{g}_k \equiv \mathcal{J}_k[F](0) = -\frac{D_k\eta_k e^{-V_k L_k/2D_k}}{\sinh(\eta_k L)}, \tag{3.48}$$

$$\bar{h}_k \equiv \mathcal{J}_k[\hat{F}](0) = D_k\eta_k\coth(\eta_k L_k) + \frac{V_k}{2}, \tag{3.49}$$

and at the primary branch

$$h_0 \equiv \mathcal{J}_0[F](L_0) = -\frac{\phi_0'(L_0)}{\phi_0(L_0)} + V_0. \tag{3.50}$$

Using these definitions the current conservation equations simplify to

$$H_{\alpha_0}\Phi_{\alpha_0} - \sum_{k\in\bar{\mathcal{I}}_{\alpha_0}} \bar{g}_k\Phi_{\alpha(k)} = \mathcal{X}_{\alpha_0} \tag{3.51}$$

for the first branch with

$$H_{\alpha_0} = h_0 - \sum_{k\in\bar{\mathcal{I}}_{\alpha_0}} \bar{h}_k. \tag{3.52}$$

Then, for $p\in\Sigma_n$, $1\le n<N$ we have

$$g_p\Phi_{\alpha'(p)} + H_{\alpha(p)}\Phi_{\alpha(p)} - \sum_{k\in\bar{\mathcal{I}}_{\alpha(p)}} \bar{g}_k\Phi_{\alpha(k)} = \mathcal{X}_{\alpha(p)}, \tag{3.53}$$

where

$$H_{\alpha(p)} = h_p - \sum_{k\in\bar{\mathcal{I}}_{\alpha(p)}} \bar{h}_k, \tag{3.54}$$

and for $p\in\Sigma_N$ we neglect the open terminal nodes so that

$$g_p\Phi_{\alpha'(p)} + H_{\alpha(p)}\Phi_{\alpha(p)} = \mathcal{X}_{\alpha(p)}. \tag{3.55}$$

Our strategy for solving this set of iterative equations will be to start at the final generation Σ_N and work inward solving recursively to branch segment j. Then we must account for terms involving $\mathcal{G}^+$ as we continue solving inward toward branch node α_0. Once Φ_0 is known we can use back substitution to obtain the remaining unknown functions. Let $\{k_m, m=1,2,\cdots,N+1\}$ be a sequence of segments starting at a node $\alpha(k_1)\in\Sigma_N$ and proceeding along a direct path toward the terminal node with $\alpha(k_{N+1})=\alpha_0$. Suppose further that the branch nodes $\beta\equiv\alpha(j)$ and $\beta'\equiv\alpha'(j)$ of the segment containing the target are contained in the set of nodes given by $\mathcal{A}\equiv\{\alpha(k_m), k=1,\ldots N+1\}$. For the moment we will assume that $j\neq 0$. Let $\alpha(k_1)$ and the nodes between $\alpha(k_1)$ and β be denoted by the set $\mathcal{A}_{\text{out}}\subset\mathcal{A}$. Similarly, let α_0 and the nodes between β' and α_0 be denoted by the set $\mathcal{A}_{\text{in}}\subset\mathcal{A}$. Hence, we have the decomposition $\mathcal{A}=\mathcal{A}_{\text{out}}+\{\beta,\beta'\}+\mathcal{A}_{\text{in}}$. Finally, let $\check{m}$ be the number of nodes contained in $\mathcal{A}_{\text{out}}$ and $\check{n}$ be the number of nodes contained in the set $\mathcal{A}_{\text{in}}$ with $\check{n}=N-\check{m}-1$. It follows that the segment containing the target is $j=k_{\check{m}+1}$ with $\beta=\alpha(k_{\check{m}+1})$ and $\beta'=\alpha(k_{\check{m}+2})$. Moreover, $\mathcal{A}_{\text{out}}=\{\alpha(k_m), m=1,\ldots,\check{m}\}$ and $\mathcal{A}_{\text{in}}=\{\alpha(k_m), m=\check{m}+3,\ldots,N+1\}$.

Starting at the outer branch node $\alpha(k_1)$ we have

$$\Phi_{\alpha(k_1)} = -\frac{g_{k_1}}{H_{\alpha(k_1)}}\Phi_{\alpha'(k_1)}. \tag{3.56}$$

Then, as we continue toward β solving recursively at branch nodes $\alpha(k_m) \in \mathcal{A}_{\text{out}}$, we have

$$\Phi_{\alpha(k_m)} = -\frac{g_{k_m}}{\hat{H}_{\alpha(k_m)}}\Phi_{\alpha'(k_m)}, \quad 1 < m \leq \check{m}, \tag{3.57}$$

where $\alpha'(k_m)=\alpha(k_{m+1})$ and the functions $\hat{H}_{\alpha(k_m)}$ are defined recursively: for $\alpha(k_2)$ we have

$$\hat{H}_{\alpha(k_2)} = H_{\alpha(k_2)} + \sum_{k' \in \bar{\mathcal{I}}_{\alpha(k_2)}} \frac{g_{k'}\bar{g}_{k'}}{\hat{H}_{\alpha(k')}}, \tag{3.58}$$

and subsequently

$$\hat{H}_{\alpha(k_m)} = H_{\alpha(k_m)} + \sum_{k' \in \bar{\mathcal{I}}_{\alpha(k_m)}} \frac{g_{k'}\bar{g}_{k'}}{\hat{H}_{\alpha(k')}}. \tag{3.59}$$

Iterating Eq. (3.59) leads to a finite continued fraction. For example, in the case of three generations ($N=3$), we have

$$\hat{H}_{\alpha_0} = H_{\alpha_0} + \sum_{k \in \bar{\mathcal{I}}_{\alpha_0}} \frac{g_k\bar{g}_k}{H_{\alpha(k)} + \sum_{l \in \bar{\mathcal{I}}_{\alpha(k)}} \frac{g_l\bar{g}_l}{H_{\alpha(l)} + \sum_{m \in \bar{\mathcal{I}}_{\alpha(l)}} \frac{g_m\bar{g}_m}{H_{\alpha(m)}}}}. \tag{3.60}$$

When we reach the node β we must account for the contributions to the current from $\mathcal{G}^+$. In particular, we now have the following inhomogeneous terms appearing in Eq. (3.53) when $\alpha(p)=\beta,\beta'$:

$$\mathcal{X}_\beta(y) = -\mathcal{J}_j[\mathcal{G}^+](L_j) = \frac{\psi_j'(0)\psi_j(y)}{W_j^+(y)}, \tag{3.61}$$

$$\mathcal{X}_{\beta'}(y) = \mathcal{J}_j[\mathcal{G}^+](0) = -\frac{\psi_j'(0)\psi_j(y-L_j)}{W_j^+(y)}. \tag{3.62}$$

We have evaluated the right-hand sides using Eq. (3.19). It follows that

$$\Phi_\beta = \frac{\mathcal{X}_\beta - g_j\Phi_{\beta'}}{\hat{H}_\beta}, \quad \Phi_{\beta'} = \frac{\hat{\mathcal{X}}_{\beta'} - g_{j'}\Phi_{\alpha'(j')}}{\hat{H}_{\beta'}}, \tag{3.63}$$

where j' is the segment for which $\alpha(j')=\beta'$, that is, $j'=k_{\check{m}+2}$, and

$$\hat{\mathcal{X}}_{\beta'} = \mathcal{X}_{\beta'} - \frac{\bar{g}_j}{\hat{H}_\beta}\mathcal{X}_\beta. \tag{3.64}$$

Continuing to iterate from β' toward α_0 the functions $\hat{\mathcal{X}}_{\alpha(k_m)}$ pick up factors of $\bar{g}_{k_m}/\hat{H}_{\alpha(k_m)}$ so that for $\alpha(k_m) \in \mathcal{A}_{\text{in}}$

$$\hat{\mathcal{X}}_{\alpha(k_m)} = \left(\prod_{i=\check{m}+2}^{m-1} \frac{\bar{g}_{k_i}}{\hat{H}_{\alpha(k_i)}}\right)\hat{\mathcal{X}}_{\beta'}, \quad m > \check{m}+2. \tag{3.65}$$

Solving recursively along these branch nodes then yields

$$\Phi_{\alpha(k_m)} = \frac{\hat{\mathcal{X}}_{\alpha(k_m)} - g_{\alpha(k_m)}\Phi_{\alpha'(k_m)}}{\hat{H}_{\alpha(k_m)}}. \tag{3.66}$$

When α_0 is reached we have

$$\Phi_{\alpha_0} = \frac{\hat{\mathcal{X}}_{\alpha_0}}{\hat{H}_{\alpha_0}}, \tag{3.67}$$

where

$$\hat{\mathcal{X}}_{\alpha_0} = \left(\prod_{i=\check{m}+2}^{N} \frac{\bar{g}_{k_i}}{\hat{H}_{\alpha(k_i)}}\right)\hat{\mathcal{X}}_{\beta'}. \tag{3.68}$$

With Φ_{α_0} known we can use back substitution to solve Eq. (3.66) along the sequence $\{k_N,k_{N-1},\ldots,k_{m+2}\}$ toward β' to get

$$\Phi_{\beta'} = \frac{1}{\hat{H}_{\beta'}}\left[\hat{\mathcal{X}}_{\beta'} + \sum_{m=0}^{\check{n}-1}\left(\prod_{i=\check{m}+2}^{N-m} \frac{-g_{k_i}}{\hat{H}_{\alpha(k_i)}}\right)\hat{\mathcal{X}}_{\alpha(k_{N+1-m})}\right]. \tag{3.69}$$

To account for the special case $j=0$ we define

$$\mathcal{Y}(y) \equiv \mathcal{J}_0[\mathcal{G}_0^-](L_0) = -\frac{\psi'(0)\phi(y)}{W^-(y)}, \tag{3.70}$$

where we have used Eq. (3.22). Since $j=0$ recurrence relation (3.57) is valid for all nodes $\alpha(k_m) \in \mathcal{A}$ except at α_0, where we have

$$\Phi_{\alpha_0} = -\frac{\mathcal{Y}}{\hat{H}_{\alpha_0}}. \tag{3.71}$$

Suppose that we wish to find the solution at the node $\alpha(k_m) \in \mathcal{A}$. Using back substitution to solve Eq. (3.57) along the sequence $\{k_N,k_{N-1},\ldots k_m\}$, $m=1,\cdots,N$, yields

$$\Phi_{\alpha(k_m)} = \left(\prod_{i=m}^{N} \frac{-g_{k_i}}{\hat{H}_{\alpha(k_i)}}\right)\Phi_{\alpha_0}. \tag{3.72}$$

The solution for Φ_α at any branch node $\alpha \in \mathcal{B}$ is now clear. Given the location of the target segment j, we have two possibilities, either $j>0$ or $j=0$. If $j>0$ then Φ_{α_0} is given by Eq. (3.67) and if $j=0$ then Φ_{α_0} is given by Eq. (3.71). Once we have Φ_{α_0} we can find $\Phi_{\alpha(k_m)}$ at any other branch node $\alpha(k_m) \in \mathcal{A}$ by using the corresponding back substitution formula (3.69) or (3.72).

C. Approximating the generating function

Given a target located on the jth branch, the calculation of the hitting probability Π and MFPT T reduces to the follow-

ing steps: (i) Calculate the Green's functions $G_{j,0}$, $G_{j,j}$ and substitute the results into the integral Eq. (3.32) for $i=j$; (ii) Solve the integral equation for $\tilde{U}_j$ and substitute into the formula for the generating function $\Upsilon_j(s)$, Eq. (3.34); (iii) Taylor expand the generating function and extract Π, T according to Eq. (3.6). That is,

$$\Pi = \Upsilon_j(0), \quad T = -\frac{\Upsilon_j'(0)}{\Upsilon_j(0)}.$$

We carry out step (ii) by numerically solving the integral equation using a standard finite-element method. We note, however, that an even simpler solution to Eq. (3.32) can be obtained in parameter regimes where $\tilde{U}_j$ is approximately constant within the target interval. Then

$$\tilde{U}_i(x,s) \approx 2\lambda \tilde{U}_j(X,s) G_{i,j}(x,X;s) - G_{i,0}(x,0;s). \quad (3.73)$$

The unknown value of $\tilde{U}_j$ at the target can be found by setting $i=j$ and $x=X$ in the above equation and solving for $\tilde{U}_j(X,s)$,

$$\tilde{U}_j(X,s) \approx \frac{-G_{j,0}(X,0;s)}{1-2\lambda G_{j,j}(X,X;s)}. \quad (3.74)$$

It follows that the generating function defined by Eq. (3.34) can be approximated as

$$\Upsilon_j(s) \approx \frac{-2\lambda G_{j,0}(X,0;s)}{1-2\lambda G_{j,j}(X,X;s)}. \quad (3.75)$$

These approximations are used to interpolate between numerical solutions of the integral equation in appropriate parameter regimes.

IV. EXAMPLES

A. Single branch

In order to illustrate the Green's function construction of Sec. III, we begin by considering a single branch node with three identical branches of length L, diffusivity D, and drift velocity V. The main branch segment ($i=0$) has a reflecting boundary at $x=0$ and a branch node at $x=L$. The two daughter branches ($i=1,2$) extending out from the branch node have open terminal nodes at $x=L$, which represent the effects of degradation or uptake by another process. At the branch node there is an unknown quantity Φ which must be determined by imposing conservation of current. It follows from Eqs. (3.37), (3.70), and (3.71) that

$$G_{0,0}(x,y) = \mathcal{G}^-(x,y) + \Phi(y)F(x) \quad (4.1)$$

and

$$G_{j,0}(x,y) = \Phi(y)\hat{F}(x), \quad j=1,2, \quad (4.2)$$

with $F(x)$, $\hat{F}(x)$ given by k-independent versions of Eq. (3.38) and

$$\Phi(y) = \frac{\psi'(0)\phi(y)}{H_0 W^-(y)}, \quad (4.3)$$

where [see Eq. (3.52)]

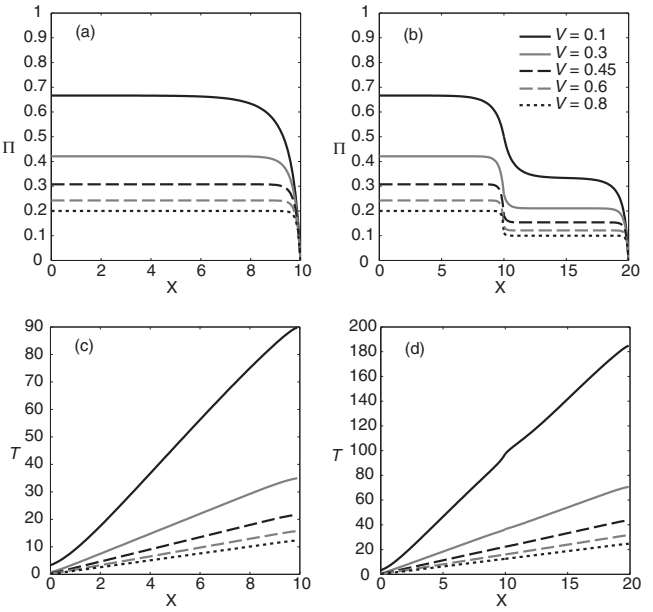

FIG. 3. The effect of a single branch on directed intermittent search. [(a), (c)] The hitting probability Π and MFPT T for a finite interval of length $2L$ (no branching) as a function of target location X and for various values of the drift velocity V. [(b), (d)] The corresponding hitting probability Π and MFPT T in the case of a single branch point at $X=L$. Nondimensional parameter values used are $L=10$, $\lambda=0.2$, and $D=0.1$.

$$H_0 = -\frac{D\phi'(L)}{\phi(L)} + V - 2\bar{h}. \quad (4.4)$$

Similarly, Eqs. (3.36) and (3.55) imply that

$$G_{j,j}(x,y) = \mathcal{G}^+(x,y) + \Phi(y)\hat{F}(x), \quad j=1,2, \quad (4.5)$$

where now

$$\Phi(y) = -\frac{\psi'(0)\psi(y-L)}{H_0 W^+(y)}. \quad (4.6)$$

Having constructed the single-branch Green's function, we can substitute the results into Eqs. (3.32) and (3.34), and use Taylor expansion (3.6) to calculate the hitting probability Π and conditional MFPT T. Plots of Π and T for both the single branch and a finite interval of length $2L$ are shown in Fig. 3. It can be seen that the absorbing boundary and the branch node affect the hitting probability by creating boundary layers. This reflects the fact that the diffusivity D is $O(\epsilon)$. As expected, the hitting probability approximately halves at the branch node. [For a branch with coordination number z, $\Pi \to \Pi/(z-1)$.] We also note that the basic qualitative behavior of Π and T as we vary the drift velocity V is similar for both the single branch [Figs. 3(b) and 3(d)] and the finite interval [Figs. 3(a) and 3(c)]. That is, as the particle slows down it is more likely to find the target, but does so at the cost of increasing the MFPT.

B. Semi-infinite Cayley tree

A dendritic tree is a highly branched structure [17]. Given the number of branches contained within a typical dendrite,

we can approximate its structure by a semi–infinite Cayley tree with coordination number $z=3$. (Extension of the analysis to $z\neq 3$ is straightforward). This approximation will be valid provided that the particle is sufficiently far from the distal ends of the tree so that boundary effects can be ignored, other than the reflecting boundary condition at the primary terminal node α_0'. We will assume for simplicity that the drift velocity V, diffusivity D, and branch length L are identical throughout the tree so that we can exploit the recursive nature of the infinite tree. (A more realistic model of a dendritic tree would need to take into account the fact that branches tend to taper as one proceeds distally away from the soma; such effects could be modeled using the general construction presented in Sec. III. However, it is not crucial in terms of the results presented in Sec. V.) Equations (3.35), (3.37), (3.71), and (3.72) imply that

$$G_{0,0}(x,y)=\mathcal{G}^{-}(x,y)+\Phi_{\alpha_0}(y)F(x) \tag{4.7}$$

and

$$G_{j,0}(x,y)=\Phi_{\beta'}(y)\hat{F}(x)+\Phi_{\beta}(y)F(x),\quad j\neq 0, \tag{4.8}$$

where

$$\Phi_{\alpha_0}(y)=\frac{\psi'(0)\phi(y)}{\hat{H}_0 W^{-}(y)}, \tag{4.9}$$

and

$$\Phi_{\beta}(y)=\left(\frac{-g}{\hat{H}}\right)\Phi_{\beta'}(y)=\left(\frac{-g}{\hat{H}}\right)^{\check{n}+1}\Phi_{\alpha_0}(y). \tag{4.10}$$

Note that the self similar structure of the tree implies that for all branch nodes $\alpha\neq\alpha_0$ we have $H_\alpha=H$ with [see Eq. (3.54)]

$$H=h-2\bar{h}=-3D\eta\cosh(\eta L)-\frac{V}{2} \tag{4.11}$$

and $\hat{H}_\alpha=\hat{H}$ with [see Eq. (3.59)]

$$\hat{H}=H+\frac{2g\bar{g}}{\hat{H}}. \tag{4.12}$$

It follows that $\hat{H}$ is the larger root of a quadratic so that

$$\hat{H}=\frac{1}{2}(H+\sqrt{H^2+8g\bar{g}}). \tag{4.13}$$

At the branch node α_0 [see Eq. (3.59)],

$$\hat{H}_0=H_0+\frac{2g\bar{g}}{\hat{H}} \tag{4.14}$$

with H_0 given by Eq. (4.4).

Similarly, Eqs. (3.35), (3.63)–(3.65), and (3.69) imply that

$$G_{j,j}(x,y)=\mathcal{G}^{+}(x,y)+\Phi_{\beta'}(y)\hat{F}(x)+\Phi_{\beta}(y)F(x) \tag{4.15}$$

for $j\neq 0$, where

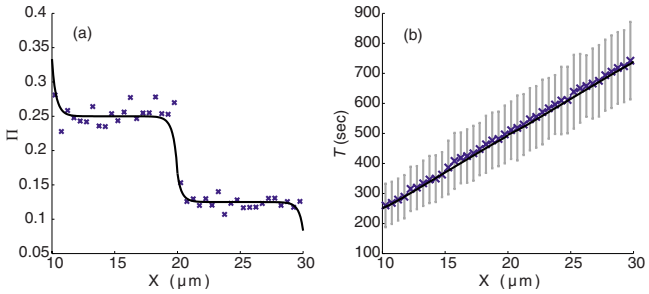

FIG. 4. (Color online) Numerical results for the hitting probability Π and MFPT T on a semi-infinite Cayley tree with coordination number $z=3$ and branch length $L=10$ μm. Comparison of Monte Carlo simulations of the full three-state Markov model with analytical results obtained for the reduced scalar FP equation. The solid gray line represents the analytical approximation of the hitting probability and MFPT obtained from the generating function (3.34). The latter is calculated by solving the integral Eq. (3.32) using the Green's function for the Cayley tree. The corresponding results from Monte Carlo simulations of the three-state model are denoted by "x." (a) The hitting probability Π as a function of the target location X. (b) The mean first passage time T as a function of the target location. (The gray bars represent the standard deviation of the first passage time evaluated using Monte Carlo simulations.) The diffusivity D, drift velocity V, and absorption rate λ of the scalar FP equation are calculated using the parameter values of the three-state model: $k=0.2$ s^{-1}, $v_{\pm}=0.2$ μm/s, $l=0.5$ μm, $\alpha=1$ s^{-1}, $\beta_+=1$ s^{-1}, and $\beta_-=2$ s^{-1}. These values are extracted from experimental values of mRNA transport in dendrites [13–16].

$$\Phi_{\beta'}(y)=\frac{1}{\hat{H}}\left[\sum_{k=0}^{\check{n}-2}\left(\frac{-g\bar{g}}{\hat{H}^2}\right)^k+\frac{\hat{H}}{\hat{H}_0}\left(\frac{-g\bar{g}}{\hat{H}^2}\right)^{\check{n}-1}\right]\hat{\mathcal{X}}_{\beta'}(y), \tag{4.16}$$

$$\Phi_{\beta}(y)=-\frac{g}{\hat{H}}\Phi_{\beta'}(y)+\frac{\psi'(0)\psi(y)}{\hat{H}W^{+}(y)}, \tag{4.17}$$

and

$$\hat{\mathcal{X}}_{\beta'}(y)=-\frac{\psi'(0)}{W^{+}(y)}\left(\psi(y-L)-\frac{\bar{g}}{\hat{H}}\psi(y)\right). \tag{4.18}$$

We have used the fact that

$$\hat{\mathcal{X}}_{\alpha(k_m)}(y)=\left(\frac{\bar{g}}{\hat{H}}\right)^{N-m}\hat{\mathcal{X}}_{\beta'}(y). \tag{4.19}$$

V. OPTIMAL SEARCH STRATEGIES

In this section we use our analytical results for a semi-infinite Cayley tree to explore the effects of branching on the efficiency of directed intermittent search. However, it is first useful to check the accuracy of our quasi-steady-state reduction by comparing our analytical results with direct Monte Carlo simulations of the full three-state Markov model (2.1). The excellent agreement between the reduced model and full model is illustrated in Fig. 4, where we plot both the hitting

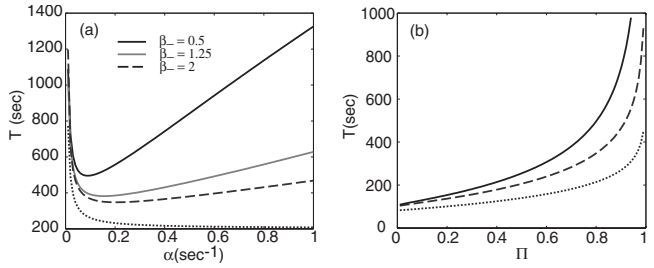

FIG. 5. MFPT on a finite interval of length $L=20$ μm with a hidden target at $X=10$ μm. (a) Plot of MFPT T as a function of α for fixed $\Pi=0.8$ and various β_-. Other parameters are $v_\pm=0.1$ μm s^{-1} and $k=0.05$ s^{-1}. Unidirectional case is shown as a dotted curve. (b) Corresponding plot of minimum search time $T_{\min}$ (with respect to variation in α) as a function of the hitting probability Π. Unidirectional case (dotted curve) is plotted for $\alpha_{\max}=0.5$ s^{-1}.

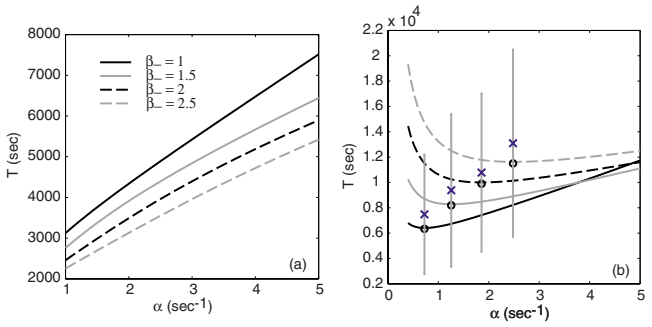

FIG. 6. (Color online) MFPT on a semi-infinite Cayley tree with coordination number $z=3$ and branch length $L=10$ μm. Target is located at a distance $X=5$ μm along a branch adjacent to the primary branch ($\check{n}=1$). (a) Plot of MFPT T as a function of α for fixed hitting probability $\Pi=0.4$ and various values of β_-. Other parameter values are $k=0.1$ s^{-1} and $v_\pm=0.1$ μm/s. (b) Corresponding plots of T for $\Pi=0.5$. The minimum MFPT for each fixed value of β_- is indicated by the black "o" mark, and the corresponding value of the MFPT obtained from Monte Carlo simulations is shown by the "x."

probability and MFPT as a function of the distance of the target from the primary terminal node (soma). Given the accuracy of our analytical approximations over physiologically reasonable parameter ranges, we now use Eqs. (3.32), (3.34), (4.7), (4.8), and (4.15) to compare the efficiency of unidirectional and bidirectional search strategies by fixing the hitting probability Π and determining the corresponding MFPT T. We will show that unlike a random search on a finite interval, there are two different regimes where different search strategies are more effective. Note that our Green's function analysis of the scalar FP Eq. (2.20) generates expressions for Π and T that depend on the diffusivity D, drift velocity V, and absorption rate λ. In order to express our results in terms of the transition rates $\alpha,\beta_\pm$ of the original three-state Markov model described by Eq. (2.1), we substitute for D,V,λ using Eqs. (2.21)–(2.23).

In the case of a one-dimensional random search, a unidirectional strategy will always find the target faster on average than a bidirectional search strategy [8]. In order to characterize the efficiency of the random search, we fix the hitting probability to some value Π_0 and numerically solve the equation $\Pi(\alpha,\beta_+,\beta_-)=\Pi_0$ for β_+. We then determine the MFPT $T(\alpha,\beta_+(\alpha,\Pi_0,\beta_-),\beta_-)$ as a function of α,β_-. The efficiency of the random search is characterized by minimizing the resulting MFPT as a function of α for different values of β_-. As we increase β_- while keeping β_+ fixed the amount of time spent in the backward moving state is decreased and the bidirectional search becomes more unidirectional. As in our previous work [8], we find that for $\beta_-<\infty$ the MFPT exhibits a unique minimum value as a function of α, and this minimum value decreases as β_- increases (see Fig. 5). Thus a unidirectional search strategy outperforms a comparable bidirectional search strategy in the one-dimensional case.

The unidirectional search strategy becomes less effective on a tree structure (with coordination number) because each time a searcher encounters a branch node, the maximum probability of finding its target is reduced by a factor of $p=1/(z-1)$. If $\check{n}$ is the number of branch nodes between the starting position and the target, then the hitting probability for a unidirectional searcher is $\Pi=\bar{\Pi}p^{\check{n}}$, where $\bar{\Pi}$ is the hitting probability for unidirectional search along a single line of the same effective length. It follows that the unidirectional hitting probability decays exponentially as a function of $\check{n}$. In order to investigate whether or not bidirectional search mitigates the effects of branching, we determine the MFPT for bidirectional search on a Cayley tree with a fixed hitting probability Π_0. First, taking $\Pi_0<p^{\check{n}}$, we find that as in the one-dimensional case, the efficiency of the random search increases as the parameter β_- is increased, see Fig. 6(a). This reflects the fact that the hitting probability is within reach of the unidirectional strategy. However, when the hitting probability crosses the critical value $p^{\check{n}}$, $\Pi_0>p^{\check{n}}$, so that a unidirectional search is no longer possible, there is a dramatic shift in the behavior of the random search, see Fig. 6(b). Now the MFPT exhibits a minimum value as a function of α and the minimum value increases rather than decreases with β_-. This observation is also confirmed by Monte Carlo simulations of the full three-state system using the transition rates corresponding to the minimum of each curve shown in Fig. 6(b). The switch between the two types of optimal behavior is further illustrated in Fig. 7.

There is another important difference between the one-dimensional case and the Cayley tree, namely, that an unbiased random walk on the tree is nonrecurrent. That is, there is a nonzero probability that even an unbiased random walker will not return to its starting point. In terms of bidirectional search biased in the forward or anterograde direction, this implies that on the Cayley tree there exists an upper bound to the hitting probability, $\Pi\leq\Pi_c<1$, where Π_c is the hitting probability for an unbiased bidirectional search. Taking the backward and forward velocities of the searcher in the three-state model (2.1) to be the same, $v_\pm=v$, an unbiased search corresponds to the condition $\beta_+=\beta_-$. In the reduced scalar model given by the FP Eq. (2.20), the unbiased case corresponds to a zero drift velocity $V=0$. In order to have $\Pi>\Pi_c$ it would be necessary for the search to be biased in the backward or retrograde direction ($V<0$), which is not consistent with motor-driven cargo transport in dendrites.

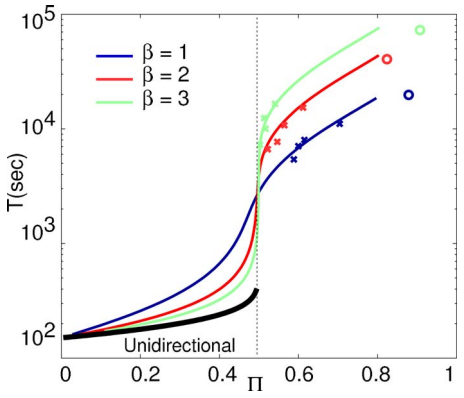

FIG. 7. (Color online) Two phases of behavior for directed intermittent search on a semi- infinite Cayley tree with coordination number $z=3$ and branch length $L=10$ μm. Target is located at a distance $X=5$ μm along a branch that is one generation away from the primary branch ($\check{n}=1$). Each thin solid curve is a parameterized plot of $[\Pi(\beta_+),T(\beta_+)]$ for fixed β_- which terminates at the point $\Pi=\Pi_c$ where the search is unbiased. [Since the accuracy of the quasi-steady-state reduction breaks down in the unbiased limit, we determine the termination points using Monte Carlo simulations (closed circles). Other points obtained from simulations are indicated by crosses.] The thick black curve represents the limiting envelope of unidirectional search. Other parameter values are $\alpha=2$ s^{-1}, $k=1$ s^{-1}, and $v_{\pm}=0.1$ μm/s.

The above results may explain why both unidirectional and bidirectional search strategies are observed in dendritic transport [13–16]. If time to target is the foremost constraint then the cell may overcome the decrease in hitting probability by inserting more resources into the dendrite. On the other hand, if production of those resources is too costly then the cell may sacrifice delivery time for more efficient localization. Thus, the two conflicting constraints are average delivery time and production cost. Even though a bidirectional search strategy can raise the hitting probability, it is clear that the hitting probability is still an exponentially decreasing function of $\check{n}$. As many dendrites are highly branched it follows that distal synapses would be extremely difficult to target from the soma. This raises the issue of whether or not the cell employs other methods to overcome this constraint. One possibility is that there are local intracellular pools of proteins and other products stored at various points along the dendrite. Interestingly, clusters of immobile transport vesicles are found at branch nodes along the dendritic tree [13–16], consistent with the notion that the dendritic tree is partitioned into smaller sub trees within which a more efficient local search strategy is performed.

VI. DISCUSSION

In this paper, we have extended our previous model of directed intermittent search [8,9] to account for the effects of branching. By using Green's function methods to derive an analytical approximation for the moment generating function, we showed that on a tree structure there are certain regimes where a bidirectional search strategy is more effective than a unidirectional one. Our results thus offer a possible explanation for the different dynamical behaviors observed in neuronal microtubular cargo transport [13–16]. We also established that branching leads to an exponential reduction in the probability of finding a distant target, suggesting that more local search strategies are necessary. This is consistent with the finding that clusters of immobile transport vesicles are found at branch nodes along the dendritic tree.

In future work we will investigate more detailed biophysical models of cargo transport, in order to take into account possible local signaling mechanisms between the target and molecular motor complex; some form of signaling could mitigate the effects of branching. Elsewhere, we have applied the quasi-steady-state reduction to a multiple motor model of bidirectional transport, in which opposing motors compete in a "tug-of-war" [35], and showed how adenosine triphosphate concentration might regulate the delivery of cargo to synaptic targets [9]. Other possible signaling molecules include microtubule associated proteins and calcium [36]. Finally, it would be interesting to develop a population-level model of the transport and delivery of cargo to multiple targets on a tree network, and the resulting competition for resources. Incorporating both global and local signaling mechanisms from synaptic targets would then allow us to explore the role of motor transport in synaptic plasticity [37] and synaptogenesis [38], for example.

ACKNOWLEDGMENT

This work was supported by the National Science Foundation (Grant No. DMS-0813677)

[1] O. Benichou, M. Coppey, M. Moreau, P. H. Suet, and R. Voituriez, Phys. Rev. Lett. **94**, 198101 (2005).
[2] O. Benichou, C. Loverdo, M. Moreau, and R. Voituriez, J. Phys.: Condens. Matter **19**, 065141 (2007).
[3] C. Loverdo, O. Benichou, M. Moreau, and R. Voituriez, Nat. Phys. **4**, 134 (2008).
[4] J. W. Bell, *The Behavioural Ecology of Finding Resources* (Chapman and Hall, London, UK, 1991).
[5] G. M. Viswanathan, S. V. Buldyrev, S. Havlin, M. G. E. da Luz, E. P. Raposo, and H. E. Stanley, Nature (London) **401**, 911 (1999).
[6] O. G. Berg, R. B. Winter, and P. H. von Hippel, Biochemistry **20**, 6929 (1981).
[7] S. E. Halford and J. F. Marko, Nucleic Acids Res. **32**, 3040 (2004).
[8] P. C. Bressloff and J. M. Newby, New J. Phys. **11**, 023033 (2009).
[9] J. M. Newby and P. C. Bressloff (unpublished).
[10] E. Messaoudi, T. Kanhema, J. Soule, A. Tiron, G. Dagyte, B. da Silva, and C. R. Bramham, J. Neurosci. **27**, 10445 (2007).

[11] K. J. De Vos, A. J. Grierson, S. Ackerley, and C. C. J. Miller, Annu. Rev. Neurosci. **31**, 151 (2008).
[12] M. P. Mattson, M. Gleichmann, and A. Cheng, Neuron **60**, 748 (2008).
[13] R. B. Knowles, J. H. Sabry, M. E. Martone, T. J. Deerinck, M. H. Ellisman, G. J. Bassell, and K. S. Kosik, J. Neurosci. **16**, 7812 (1996).
[14] M. S. Rook, M. Lu, and K. S. Kosik, J. Neurosci. **20**, 6385 (2000).
[15] J. Dynes and O. Steward, J. Comp. Neurol. **500**, 433 (2007).
[16] B. Cui, C. Wu, L. Chen, A. Ramirez, E. L. Bearer, W.-P. Li, W. C. Mobley, and S. Chu, Proc. Natl. Acad. Sci. U.S.A. **104**, 13666 (2007).
[17] G. Stuart, N. Spruston, and M. Hausser, *Dendrites* (Oxford University Press, Oxford, UK, 2007).
[18] J. Koplik, S. Redner, and D. Wilkinson, Phys. Rev. A **37**, 2619 (1988).
[19] P. C. Bressloff, V. M. Dwyer, and M. J. Kearney, J. Phys. A **29**, 6161 (1996).
[20] P. C. Bressloff, V. M. Dwyer, and M. J. Kearney, Phys. Rev. Lett. **77**, 5075 (1996).
[21] C. W. Gardiner, *Handbook of Stochastic Methods for Physics, Chemistry, and the Natural Sciences*, 4th ed. (Springer-Verlag, Berlin, 2007).
[22] E. A. Brooks, Ann. Appl. Probab. **9**, 719 (1999).
[23] A. Friedman and G. Craciun, SIAM J. Math. Anal. **38**, 741 (2006).
[24] M. C. Reed, S. Venakides, and J. J. Blum, SIAM J. Appl. Math. **50**, 167 (1990).
[25] S. Redner, *A Guide to First-Passage Processes* (Cambridge University Press, Cambridge, UK, 2001).
[26] E. G. Butz and J. D. Cowan, Biophys. J. **14**, 661 (1974).
[27] B. Horwitz, Biophys. J. **36**, 155 (1981).
[28] C. Koch and T. Poggio, J. Neurosci. Methods **12**, 303 (1985).
[29] W. R. Holmes, Biol. Cybern. **55**, 115 (1986).
[30] L. F. Abbott, E. Fahri, and S. Gutmann, Biol. Cybern. **66**, 49 (1991).
[31] B. J. Cao and L. F. Abbott, Biophys. J. **64**, 303 (1993).
[32] P. C. Bressloff, V. M. Dwyer, and M. J. Kearney, J. Phys. A **29**, 1881 (1996).
[33] S. Coombes, Y. Timofeeva, C. M. Svensson, G. J. Lord, K. Josic', S. J. Cox, and C. M. Colbert, Biol. Cybern. **97**, 137 (2007).
[34] P. C. Bressloff, Phys. Rev. E **79**, 041904 (2009).
[35] M. J. I. Müller, S. Klumpp, and R. Lipowsky, Proc. Natl. Acad. Sci. U.S.A. **105**, 4609 (2008).
[36] A. Y. N. Goldstein, X. Wang, and T. L. Schwarz, Curr. Opin. Neurobiol. **18**, 495 (2008).
[37] C. R. Bramham and D. G. Wells, Nat. Rev. Neurosci. **8**, 776 (2007).
[38] C. Waites, A. Craig, and C. Garner, Annu. Rev. Neurosci. **28**, 251 (2005).